Rev. Roum. Sci. Techn.– Électrotechn. et Énerg.
Vol. **63**, *1*, pp. 33–37, Bucarest, 2018

Dedicated to the memory of Academician Andrei Țugulea

ELECTROMAGNETIC ANALYSIS OF A HYBRID PERMANENT MAGNET GENERATOR

TIBERIU TUDORACHE[1], LEONARD MELCESCU[1], VALERIU BOSTAN[1],
GABRIEL COLȚ[1], MIHAIL POPESCU[2], MIHAI PREDESCU[3]

Key words: Electromagnetic field analysis, Finite element method, Hybrid permanent magnet generator.

This paper deals with the numerical analysis of a hybrid permanent magnet generator able to produce simultaneously electric and thermal energy being dedicated for wind conversion systems. The studied machine is equipped with permanent magnets and it is analyzed from electromagnetic point of view using 2D and 3D finite element numerical models developed in Flux software package. The purpose of the analysis is to estimate the performance and operation characteristics of the machine. The numerical results are experimentally validated by measurements on a prototype.

1. INTRODUCTION

Wind power is one of the most abundant forms of renewable resources available on our planet, its exploitation being a priority for most countries of the world [1, 2].

A key component of a wind conversion system is the *electric generator* whose role is to convert mechanical energy into electricity. Various synchronous and induction generators are proposed for wind turbines [3–8].

This paper analyzes a special hybrid permanent magnet generator (HPMG) which is able to convert the rotational mechanical energy simultaneously into electricity and heat.

HPMG is a two in one machine that includes a permanent magnet synchronous generator (PMSG) and a permanent magnet heater (PMH) Fig. 1 [9–14]. The PMSG is classical except the steel tube mounted around the stator core on which a copper tube serpentine is brazed, Fig. 1. A liquid thermal agent flows through the serpentine with the purpose to recuperate a part of the losses (iron losses, Joule losses, etc.) dissipated in PMSG.

PMH includes a rotor equipped with PMs and a stator represented by the same steel tube of the PMSG which is properly extended. By spinning the rotor, the magnetic field generated by the PMs induces eddy currents in the stator tube that are converted into heat and recuperated, in most part, by the thermal agent flowing through the serpentine.

HPMG is a cogeneration device that operates at high efficiency values since a large part of PMSG losses are recuperated by the thermal fluid agent. For high efficiency and minimum thermal losses such generators could be integrated in direct drive small power wind conversion systems mounted near the end users (e.g. near the buildings or on their rooftop). Since the heat is evacuated from the HPMG by forced convection, the machine can be downsized compared to classical electric generators for the same performance, resulting a high energy density machine.

The numerical analysis of the HPMG as well as the estimation of its operation characteristics are carried out based on the finite element method (FEM) using the professional software package Flux ® [15]. The machine is analyzed from electromagnetic point of view and the numerical results are experimentally validated.

2. MAIN DATA OF STUDIED HPMG

The studied HPMG has a rated total power $P_n = 3$ kW (2.4 kW electric power and 0.6 kW thermal power), a rated voltage $V_n = 195$ V, a rated current $I_n = 7.1$ A, a rated speed $n_n = 230$ rpm. The PMSG has $2p = 38$ poles and its stator magnetic core is made of electric steel laminations with 48 slots. The PMH has $2p = 12$ poles and its stator is represented by a steel tube where eddy currents are developed. On the outer surface of the steel tube a copper tube serpentine of 8 mm outer diameter is soldered. The PMs are made of NdFeB (with remnant flux density $B_r = 1.17$ T and relative magnetic permeability $\mu_r \approx 1.088$).

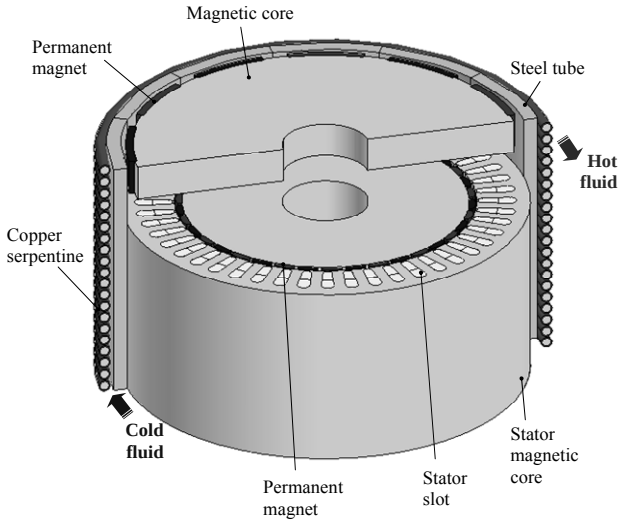

Fig. 1 – Main parts of the studied HPMG (3D cutaway view).

Some geometrical data of the HPMG (PMSG and PMH) are given in Table 1.

Table 1

Main geometrical data of the HPMG

Outer diameter of steel tube [mm]	305
Inner diameter of steel tube [mm]	285
Bore diameter of PMSG [mm]	210
Axial length of PMSG [mm]	130
Axial length of PMH [mm]	25
Outer diameter of copper tube [mm]	8

[1] "Politehnica" University of Bucharest, Electrical Engineering Faculty, Bucharest, E-mail: tiberiu.tudorache@upb.ro
[2] Research Institute for Electrical Engineering (ICPE-CA), Bucharest, E-mail: pd_mihail@yahoo.com
[3] Aeolus Energy International, Bucharest, E-mail: predescu@aeolusenergy.ro

3. ELECTROMAGNETIC FIELD MODELS

Taking into account the special construction of the HPMG which is a *two in one machine*, its analysis from electromagnetic point of view can be split into two parts. The first part of the FEM analysis that refers to the PMSG will be done by a 2D approach (for CPU time reduction reasons) and the second part of the analysis that refers to the PMH will be based on a 3D approach due to the eddy currents distribution that has a 3D pattern.

3.1. ELECTROMAGNETIC FIELD MODEL OF PMSG

The study of PMSG by FEM supposes a 2D transient magnetic field analysis using step-by-step in time domain method characterized by the following partial differential equation expressed in magnetic vector potential **A** [15]:

$$\mathrm{rot}\left[\nu(\mathbf{B})\,\mathrm{rot}\,\mathbf{A}-\mathbf{H_c}\right]=\mathbf{J} \tag{1}$$

where ν is the magnetic reluctivity, **J** is the current density flowing through the stator coils and $\mathbf{H_c}$ is the coercive magnetic field of PMs (PMs are characterized also by remnant magnetic flux density $\mathbf{B_r}$).

In order to determine the current density **J** corresponding to the stator coils in (1), which is apriori unknown, the FEM model of the PMSG is associated to an equivalent three-phase circuit model of the machine [16].

By taking into account the geometrical and physical symmetries the 2D FEM computation domain is reduced to half of the PMSG cross-section, as shown in Fig. 2, where the FE discretization is also illustrated.

The solution uniqueness of (1) is ensured by imposing Dirichlet boundary condition on the outer and inner frontiers of the computation domain in Fig. 2 and anti-cyclical boundary conditions on its radial frontiers.

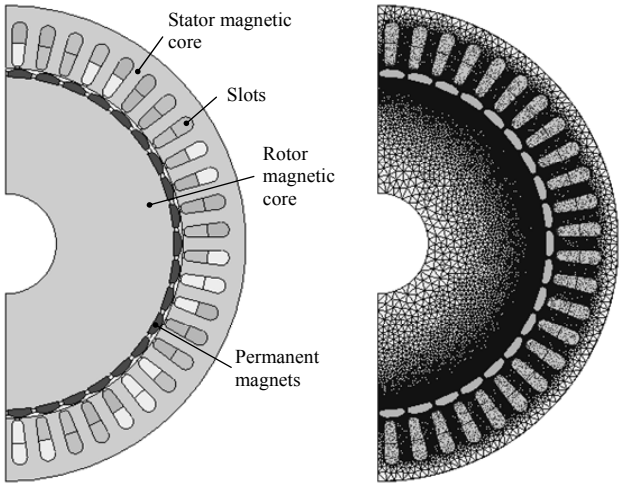

Fig. 2 – Computation domain and FE discretization of PMSG.

3.2. ELECTROMAGNETIC FIELD MODEL OF PMH

The eddy currents induced in the stator steel tube of PMH have a 3D spatial distribution. That is why a 3D FEM analysis of this component of the HPMG is compulsory. This study supposes also a transient magnetic field analysis of the device by the step-by-step in time domain method. The transient magnetic field model $\mathbf{T}\Phi-\Phi$ based on total magnetic scalar potential Φ and electric vector potential **T** formulations is described by the following general partial differential equation [15]:

$$\mathrm{div}\left[\mu(-\mathrm{grad}\,\Phi+\mathbf{T})+\mathbf{B_r}\right]=0 \tag{2}$$

By taking into account the geometrical and physical symmetries of the PMH the 3D computation domain is confined to only 2 magnetic poles, as shown in Fig. 3. The open boundary conditions are imposed by the *infinite box* feature implemented in Flux software package [15].

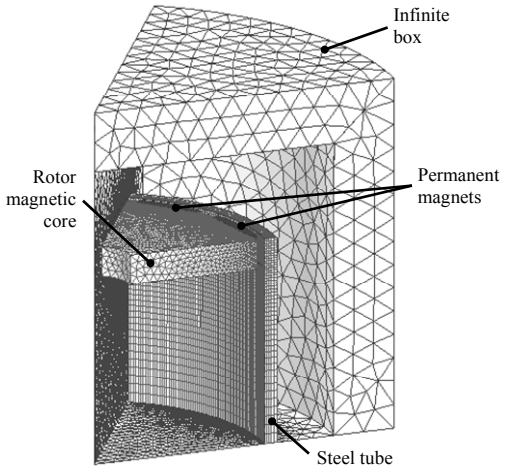

Fig. 3 – Computation domain and FE discretization of PMH.

4. NUMERICAL RESULTS

4.1. NUMERICAL RESULTS FOR PMSG

The numerical simulations allowed estimating the voltage – speed characteristic in no–load operation and the external characteristic of the PMSG for *R* and *L* type loads, Figs. 4 and 5.

The oscillations of the electromagnetic torque as well as the current and voltage waveforms were also determined, Figs. 6–8.

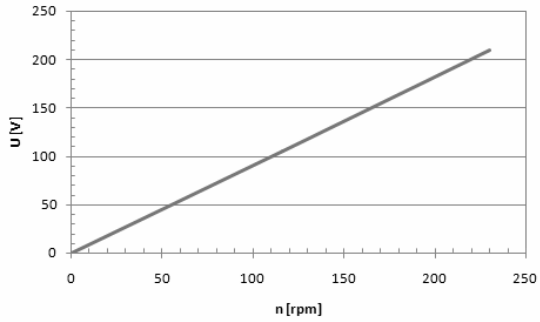

Fig. 4 – Voltage – speed characteristic of PMSG in no-load operation.

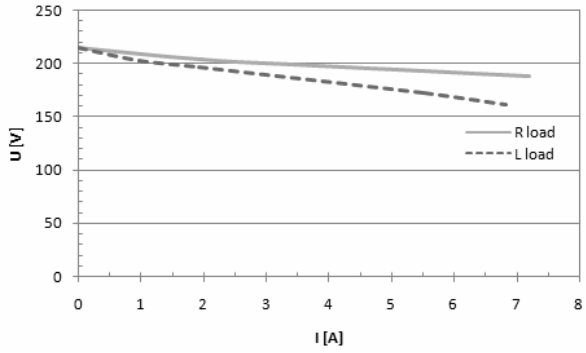

Fig. 5 – External characteristics of PMSG for *R* and *L* types loads.

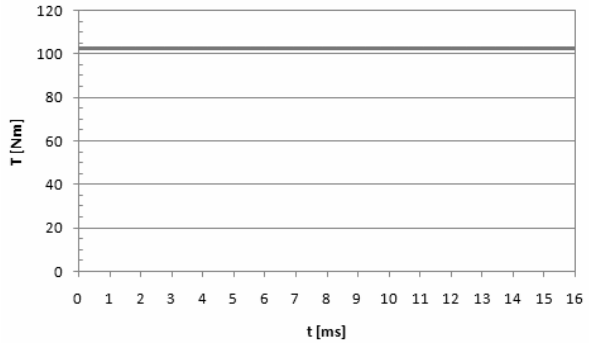

Fig. 6 – Electromagnetic torque oscillations of PMSG for rated load.

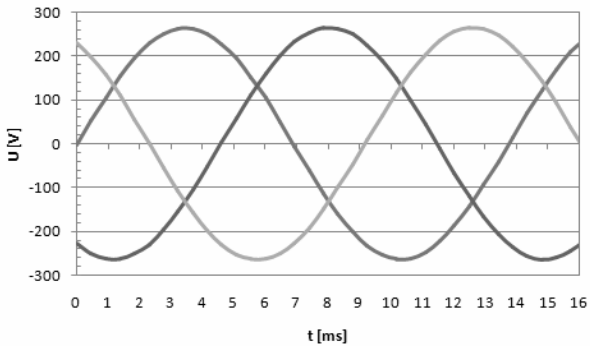

Fig. 7 – Time variations of line voltages of PMSG under load.

By studying the results in Fig. 4 we can notice a linear increase of the electromagnetic torque with the rotor speed of PMSG.

The external characteristics of the PMSG for *R* and *L* loads, shown in Fig. 5, are decreasing with the load current. From no load to full load the voltage drop is of about 12.5 % for *R* load and 25.6 % for *L* load.

The time variation of electromagnetic torque represented in Fig. 6 reveals very small torque oscillations, less than 0.74 %. The waveforms of line voltages of the PMSG shown in Fig. 7 are very close to perfect sinusoidal signals.

4.2. NUMERICAL RESULTS FOR PMH

The 3D transient magnetic field analysis of the PMH allowed us to determine various quantities and characteristics of the heater such as: distribution of magnetic flux density and induced power density in the steel tube (Fig. 8), the torque – speed characteristic (Fig. 9), and the electromagnetic torque oscillations (Fig. 10).

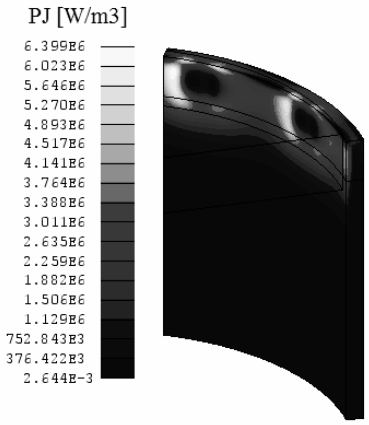

Fig. 8 – Map of induced power density in the steel wall of HPMG.

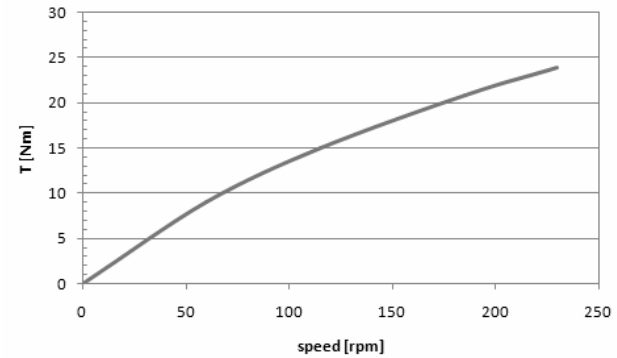

Fig. 9 – Torque speed characteristic of PMH.

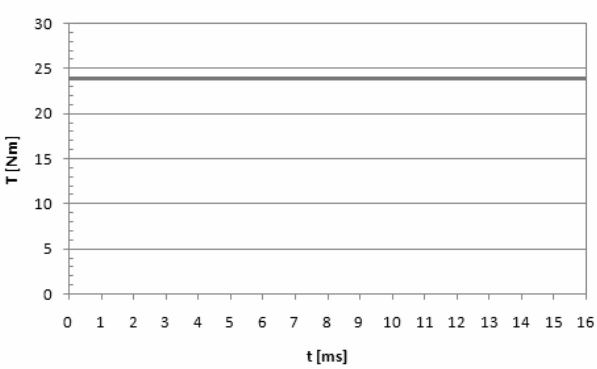

Fig. 10 – Electromagnetic torque oscillations of PMH.

As we can see in Fig. 9, the electromagnetic torque of PMH increases almost linearly with the rotor speed. The numerical results shown in Fig. 10 reveal negligible electromagnetic torque oscillations of PMH. By summing the results shown in Figs. 6 and 10 we can conclude that electromagnetic torque ripples of the PMHG are very small.

5. EXPERIMENTAL RESULTS. VALIDATION OF NUMERICAL RESULTS

The numerical results were validated by measurements carried out on the experimental model of the HPMG shown in Fig. 11.

The diagram of the experimental setup is shown in Fig. 12 where we can identify the driving system represented by an inverter fed induction motor, a gearbox, the HPMG, and the management system for the electric and thermal energy.

As we can see the experimental setup includes also a torque and speed sensor and the power electronics modules for the grid connection of the HPMG.

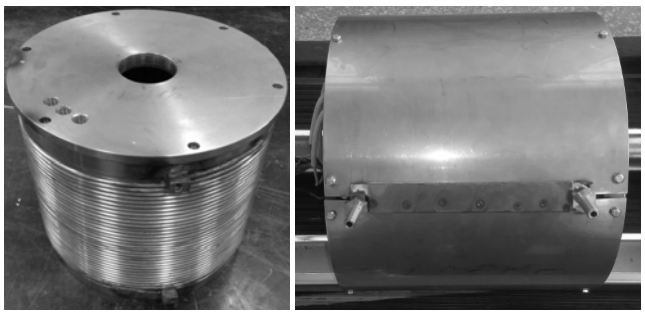

a) b)

Fig. 11 – Experimental model of HPMG: a) HPMG without cover (copper serpentine is visible); b) full HPMG prototype.

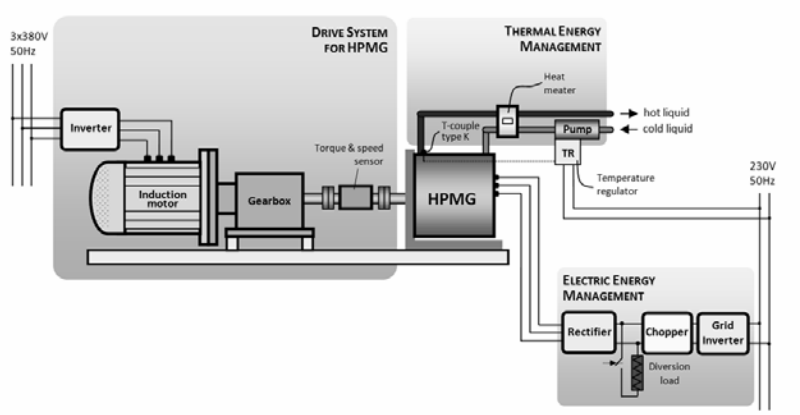

Fig. 12 – Diagram of experimental setup.

The experimental setup installed at "Politehnica" University of Bucharest for measurements is shown in Fig. 13 where we can identify the HPMG, the induction motor and the gearbox used to drive the generator. The rectifier and the inverter to connect the generator to the grid is also shown.

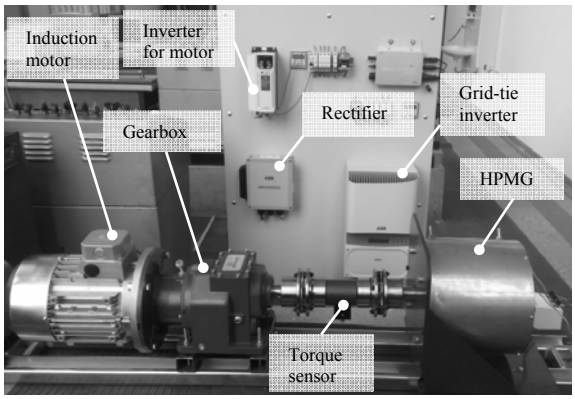

Fig. 13 – Experimental setup used for measurements.

The experimental measurements allowed validating a part of the numerical results. In Fig. 14 is shown a comparison between the numerical and experimental results regarding the external characteristic of the PMSG. A good agreement between the results can be noticed.

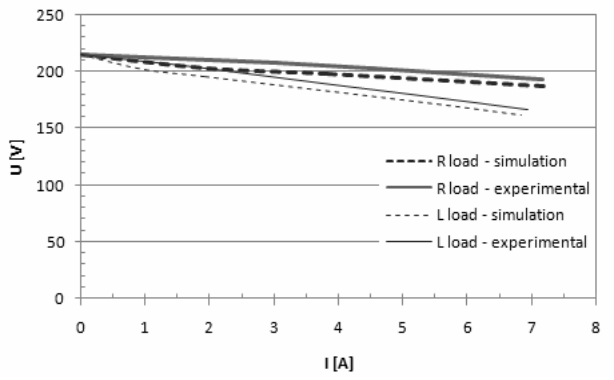

Fig. 14 – External characteristics of PMSG for *R* and *L* type loads.

Other experimental results are shown in Figs. 15 and 16 where are presented the time variations of phase current of HPMG (with the rectifier connected to its terminals) and the current injected by the inverter to the grid.

We can notice that the HPMG phase current in Fig. 15 has an important harmonics content due to the presence of the diode rectifier connected to the generator terminals.

The harmonics content of the current injected by the inverter to the grid shown in Fig. 16 is smaller.

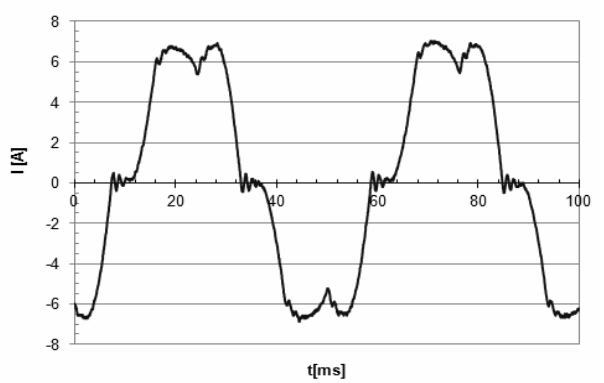

Fig. 15 – Time variation of HPMG phase current when the rectifier is connected to its terminals.

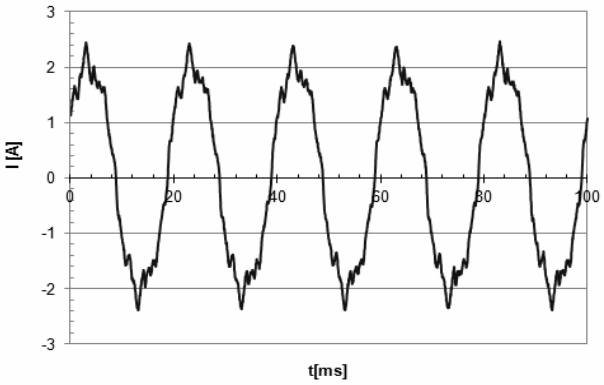

Fig. 16 – Time variation of the current injected by the inverter to the grid.

The global efficiency η_{PMHG} of PMHG that takes into account both electric and thermal powers was determined experimentally by using the following expression:

$$\eta_{PMHG} = 100 \cdot (P_{el} + P_{th})/(P_{mec} + P_{pump}), \qquad (3)$$

where $P_{el} = \sqrt{3}VI \cos \varphi$ is the output active power of PMHG, P_{th} is the thermal power measured with a heat meater, P_{mec} is the input mechanical power received by the generator at its shaft measured with a KTR 32/300 torque-speed sensor and P_{pump} is the average power absorbed by the pumping system.

The following measurement results were obtained for an operation point close to the rated one: $P_{el} = 2409$ W,

(V = 193.9 V, I = 7.23 A, cos φ = 1 for resistive load), P_{th} = 624 W, P_{mec} = 3335 W, $P_{pump} \approx$ 25 W. Thus the global efficiency of the PMHG is:

$$\eta_{HWG} = 100 \cdot (2409 + 624)/(3335+25) = 90.27\ \% \quad (4)$$

Such an efficiency value is significantly above those of classical PM generators of the same range of power and speed since the losses of common electric generators are not recuperated.

The ratio between electric and thermal powers (P_{el}/P_{th}) for the rated operation point of the studied hybrid generator is close to 4. Depending on the imposed specifications this ratio can be adjusted by a proper design of the machine.

6. CONCLUSIONS

This paper dealt with the numerical analysis of a HPMG from electromagnetic point of view. The studied machine is designed for small power grid tie wind turbines. The 2D and 3D FE simulations allowed the estimation of the machine performance and specific operation characteristics.

The numerical results were validated by experimental measurements, the agreements between the results being good.

The HPMG was proved to be a well designed machine characterized by very small torque ripples and very high global (electric and thermal) efficiency.

ACKNOWLEDGEMENTS

This paper was partly supported by the Bridge Grant Programme – PNCDI III, financed by UEFISCDI, project no. 68BG/2016.

Received on November 7, 2017

REFERENCES

1. ***, *Global Wind Report Annual Market Update: 2016*, Global Wind Energy Council, 2016.
2. ***, *Global Wind Statistics 2016*, Global Wind Energy Council (GWEC), February 2017.
3. S. Tamalouzt, K. Idjdarene, T. Rekioua, R. Abdessemed, *Direct Torque Control of Wind Turbine Driven Doubly Fed Induction Generator*, Rev. Roum. Sci. Techn.– Électrotechn. et Énerg., **61**, *3*, pp. 244–249 (2016).
4. A. Kerboua, M. Abid, *Hybrid Fuzzy Sliding Mode Control of a Doubly-Fed Induction Generator in Wind Turbines*, Rev. Roum. Sci. Techn.– Électrotechn. et Énerg., **57**, *4*, pp. 412–421 (2012).
5. L. Barote, C. Marinescu, *Modeling and Operational Testing of an Isolated Variable Speed PMSG Wind Turbine with Battery Energy Storage*, Advances in Electrical and Computer Engineering Journal, **12**, *2*, pp. 81–88 (2012).
6. N. S. Patil, Y. N. Bhosle, *A review on wind turbine generator topologies*, Proc. of International Conference on Power, Energy and Control (ICPEC), India, 2013.
7. K. Ahsanullah, R. Dutta, M.F. Rahman, *Review of PM generator designs for direct-drive wind turbines*, Proc. of 22nd Australasian Universities Power Engineering Conference (AUPEC), Indonesia, 2012.
8. L.L. Amuhaya, M.J. Kamper, *Design by optimisation of a buried PM variable-flux wind generator for grid connection*, Proc. of International Conference on Optimization of Electrical and Electronic Equipment (OPTIM) & 2017 International Aegean Conference on Electrical Machines and Power Electronics (ACEMP), Romania, 2017.
9. T. Tudorache, I. Trifu, D. Floricau, *Numerical Analysis of an Electro-Thermal Wind Generator*, Proc. of the 9th International Conference on Electronics, Computers and Artificial Intelligence (ECAI), Romania, 2017.
10. T. Tudorache, L. Melcescu, M. Predescu, *Analysis of a Permanent Magnet Eddy Current Heater Driven by a Wind Turbine*, Advances, Electrical and Computer Engineering Journal, **15**, *3*, pp. 53–58 (2015).
11. T. Tudorache, M. Popescu, *FEM Optimal Design of Wind Energy-based Heater*, Acta Polytechnica Hungarica, **6**, *2*, pp. 55–70, (2009).
12. T. Tudorache, L. Melcescu, M. Predescu, S. Nicolaie, M. Popescu, *Hybrid wind generator with radial magnetic flux and outer rotor*, Patent demand CBI A/00838/10.11.2014 under evaluation at OSIM, 2014.
13. T. Tudorache, M. Predescu, S. Nicolaie, M. Popescu, *Hybrid wind generator with radial magnetic flux and inner rotor,* Patent demand CBI A/00839/10.11.2014 under evaluation at OSIM, 2014.
14. T. Tudorache, M. Predescu, S. Nicolaie, M. Popescu, *Hybrid wind generator with axial magnetic flux*, Patent demand CBI A/00840/10.11.2014, under evaluation at OSIM, 2014.
15. Cedrat, *User guide Flux® 11*, 2015.
16. T. Tudorache, L. Melcescu, D. Floricau, *Design and Performance Analysis of a Permanent Magnet Synchronous Generator Equipped with AC-DC Converter,* Proc. of 9th International Symposium on Advanced Topics in Electrical Engineering (ATEE 2017), Romania, 2015.